Chin. J. Astron. Astrophys. Vol. 5 (2005), No. 3, 229–237
(*http://www.chjaa.org*)

Chinese Journal of
Astronomy and
Astrophysics

The Correlation between Gamma-ray and Radio Emissions in γ-ray Loud Blazars *

Jiang-He Yang[1,2] and Jun-Hui Fan[2,3,4]

[1] Department of Physics and Electronics Science, Hunan University of Arts and Science, Changde 415000; *fjh@gzhu.edu.cn; yjianghe@163.com*
[2] Center for Astrophysics, Guangzhou University, Guangzhou 510405
[3] National Astronomical Observatories, Chinese Academy of Sciences, Beijing 100012
[4] Physics Institute, Hunan Normal University, Changsha 410081

Received 2004 August 30; accepted 2005 March 5

Abstract We collect 119 γ-ray-loud blazars (97 flat spectrum radio quasars (FSRQs) and 22 BL Lacertae objects (BL Lacs)), and investigate possible correlations between their γ-ray emission (maximum, minimum and average values) at 1 GeV and the radio emission at 8.4 GHz. Our main results are as follows. For the lower state γ-ray data, there is no correlation between the γ-ray and radio flux density; For the high state γ-ray data, there are good correlations for the whole 119 blazars and 97 FSRQs, and a weak correlation for the 22 BL Lac objects; For the average γ-ray data, there are good correlations. According to our analysis, we propose that the γ-rays are associated with the radio emission from the jet, and that the γ-ray emission is likely from the SSC process in this case.

Key words: Galaxies: active — BL Lacertae objects — quasars

1 INTRODUCTION

One of the important discoveries of CGRO/EGRET instrument in extragalactic astronomy is that blazars (flat spectrum radio quasars or FSRQs, and BL Lac objects) emit most of their bolometric luminosity in the high γ-ray energy range (E >100 MeV). Many γ-ray blazars are also superluminal radio sources (Von Montigny et al. 1995). Up to now, many blazars detected by EGRET have been identified (Fichtel et al. 1994; Thompson et al. 1995; Hartman et al. 1999). The Whipple Observatory has detected three BL Lac objects above 300 GeV; they are Mrk 421 (Punch et al. 1992), Mrk 501 (Quinn et al. 1996), and PKS 2344+514 (Catanese et al. 1998), the last one has not been detected by EGRET. The γ-ray flux of blazars dominates over the flux in lower energy bands, and its luminosity above 100 MeV ranges from less than

* Supported by the National Natural Science Foundation of China.

3×10^{44} erg s^{-1} to more than 10^{49} erg s^{-1}. Many of the sources are strongly variable in the γ-band on timescales from days to months.

At present, the origin of the strongly variable emission is still not clear. Various models have been proposed for the γ-ray emissions. These models include mainly the synchrotron self-Compton model (SSC), in which the soft photons originate as synchrotron emission in the jet (Maraschi et al. 1992). The Inverse Compton processes on the external photons, in which soft photons come directly from a nearby accretion disk (Dermer et al. 1992) or from the disk radiation reprocessed in some region of the AGN (Blandford & Levinson 1995). Synchrotron emission from ultra-relativistic electrons and positrons is produced in a proton-induced cascade (PIC) (Mannheim & Biermann 1992; Cheng & Ding 1994). However, none of these models has proved convincing.

It is well known that various relations among the emissions of different wave bands might be used to distinguish the variety of emission mechanisms. Dondi & Ghisellini (1995) found that the γ-ray luminosity is correlated with the radio luminosity more than with any other band. However, Mücke et al. (1997) found no such correlation between the γ-ray and the radio bands. Fan (1997) has investigated the correlation between the γ-ray band and the lower energy bands by means of multiple regression. He found that there is an indication of a correlation between the γ-ray flux and the radio flux while there is no correlation between the γ-ray flux and the optical flux or the x-ray flux. Moreover, Fan (1997) proposed that the γ–radio correlation is probably duo to the fact that 1) both the γ-ray and the radio emissions are strongly beamed and the γ-ray emission is from the SSC process; 2) the reason for the different results is that the lower frequency radio emissions are not all from the jets, in addition that radio and the γ-ray emissions are both variable (Von Montigny et al. 1995, see also Hartman 1996). Therefore, simultaneous multi-wavelength observations and the variability in various bands are important for investigating the γ-ray—radio correlation. However, it is difficult to achieve simultaneous multi-band observations, and we have to resort to using data relating to different states (the high and low state data and the average data) to investigate the existence of correlation between γ-ray and radio emission. In this paper, we will investigate in detail the correlations for a sample of 119 blazars.

2 DATA AND RESULTS OF ANALYSIS

2.1 Data

All the collected data and their sources are listed in Table 1. There are 119 γ-ray loud blazars. In Table 1, Col.1 (3EG) gives the name of the 3EG source; Col.2 (ID (f,b)), other names of the identified source and the classification of blazar (f=flat spectrum radio quasars (FSRQs), b=BL Lac object); Col.3 (z), the redshift; Col.4 ($F_{8.4\mathrm{GHz}}$), the 8.4 GHz flux density in units of Jy ; Col.5 ($\alpha_{\mathrm{R}}^{8.4\mathrm{GHz}}$) the spectral index of the radio emission at 8.4 GHz; Col.6 (Ref.), references for $F_{8.4\mathrm{GHz}}$ data; Col. 7, 8 and 9 give, respectively ($N_{\gamma\mathrm{max}}$, $N_{\gamma\mathrm{min}}$, and $N_{\gamma\mathrm{ave}}$), the observed maximum (high state), minimum (lower state) and average γ-ray photon flux (> 100 MeV) in units of 10^{-8} photon cm^{-2} s^{-1}; and Col.10, (α_{G}), the γ-ray spectral index. Of the 119 blazars, 97 are FSRQs, 22 are BL Lac objects.

2.2 Method of Analysis

To investigate in detail the correlation between the γ-ray and radio flux density, we will classify the data in Table 1 into two groups, namely FSROs (f) and BL Lac's (b).

For each group we use the maximum, minimum and average γ-ray flux to study possible correlations between the the γ-ray at 1 GeV and the radio emission at 8.4 GHz. First, the

Table 1 A Sample of γ-ray Loud Blazars with Radio Emission at 8.4 GHz

3EG	ID (f, b)	z	$F_{8.4}$/Jy	$\alpha_{\rm R}$	Ref.	$N_{\gamma{\rm max}}$	$N_{\gamma{\rm min}}$	$N_{\gamma{\rm ave}}$	$\alpha_{\rm G}$
J0038–0949	J0039−0942 (f)	2.101	0.187	–0.12	S04	37.7	21.6	12.0	1.70
J0118+0248	J0122+0310 (f)	4.00	0.121	–0.1	S02	20.3	20.3	5.1	1.63
J0118+0248	J0121+0422,0119+041 (f)	0.63	1.351	–0.1	S02	20.3	20.3	5.1	1.63
J0130–1758	J0132–1654 (f)	1.020	0.952	–0.08	S04	13.8	13.3	11.6	1.50
J0204+1458	J0204+1514,0202+149 (f)	0.41	3.325	0.09	S02	52.8	23.6	8.7	1.23
J0215+1123	J0213+1213 (b)	0.25	0.164	–0.1	S02	18.0	18.0	4.6	1.03
J0222+4253	J0222+4302,0219+428 (b)	0.44	0.728	0.17	S02	25.3	14.8	18.7	1.01
J0237+1635	J0238+1636,0235+164 (f)	0.94	5.453	–0.5	S02	65.1	12.0	25.9	0.85
J0239+2815	J0237+2848,0234+285 (f)	1.21	3.123	–0.1	S02	31.4	16.2	13.8	1.53
J0245+1758	J0242+1742 (f)	0.55	0.236	–0.1	S02	25.9	22.8	8.8	1.61
J0245+1758	J0246+1823 (f)	3.59	0.125	0.29	S02	25.9	22.8	8.8	1.61
J0329+2149	J0325+2224,0322+222 (f)	2.07	0.528	0.0	S02	29.1	16.3	7.4	1.61
J0340–0201	J0339–0133 (f)	3.182	0.339	0.28	S04	177.6	47.4	15.1	0.84
J0340–0201	J0339–0146 (f)	0.852	3.010	–0.13	S04	177.6	47.4	15.1	0.84
J0404+0700	J0406+0637 (f)	0.67	0.227	0.0	S02	24.3	23.2	11.1	1.65
J0404+0700	J0407+0742 (b)	1.13	0.524	–0.3	S02	24.3	23.2	11.1	1.65
J0404+0700	J0409+0640 (f)	0.81	0.181	–0.1	S02	24.3	23.2	11.1	1.65
J0412–1853	J0409–1948 (f)	1.986	0.108	0.11	S04	49.5	49.5	4.5	2.25
J0412–1853	J0416–1851 (f)	1.536	0.780	0.23	S04	49.5	49.5	4.5	2.25
J0422–0102	J0423–0120 (f)	0.915	4.250	–0.2	S04	50.2	15.2	16.3	1.44
J0423+1707	J0422+1741 (f)	0.91	0.131	–0.5	S02	46.5	18.3	15.8	1.43
J0442–0033	J0442–0017 (f)	0.844	0.860	0.39	S04	85.9	47.7	12.5	1.37
J0450+1105	J0448+1127 (f)	1.37	0.206	0.17	S02	109.5	17.7	14.9	1.27
J0456–2338	J0457–2324 (f)	1.003	1.850	0.0	S04	14.7	14.7	8.1	2.14
J0459+0544	J0457+0645 (f)	0.41	0.434	0.07	S02	34.0	16.7	6.1	1.36
J0459+0544	J0502+0609,0459+060 (f)	1.11	0.543	0.28	S02	34.0	16.7	6.1	1.36
J0459+0544	J0505+0459 (f)	0.95	0.808	0.10	S02	34.0	16.7	6.1	1.36
J0500–0159	J0501–0159 (f)	2.286	3.700	–0.25	S04	31.7	11.8	11.2	1.45
J0510+5545	J0514+5602 (f)	2.19	0.229	0.18	S02	55.6	18.6	21.3	1.19
J0530–3626	J0522–3627 (b)	0.061	5.000	0.63	S04	31.9	20.2	15.8	1.63
J0530+1323	J0530+1331,0528+134 (f)	2.07	3.074	–0.3	S02	351.4	32.4	93.5	1.46
J0531–2940	J0539–2839 (f)	3.104	0.760	0.06	S04	35.0	18.6	6.9	1.47
J0533+4751	J0533+4822,0529+4820 (f)	1.16	0.556	–0.1	S02	32.7	17.2	14.0	1.55
J0542+2610	J0540+2507 (f)	0.62	0.207	0.12	S02	74.0	17.2	14.7	1.67
J0737+1721	J0738+1742,0735+178 (b)	0.42	2.942	–0.1	S02	29.3	20.4	16.4	1.60
J0743+5447	J0742+5444,0738+5451 (f)	0.72	0.142	0.36	S02	42.1	11.4	11.1	1.03
J0808+4844	(0804+499) (f)	1.43	0.880	0.12	S02	15.1	10.1	10.7	1.15
J0808+5114	J0807+5117,0803+5126 (f)	1.14	0.358	–0.4	S02	23.4	15.9	8.7	1.76
J0808+5114	J0809+5218 (b)	0.14	0.154	0.08	S02	23.4	15.9	8.7	1.76
J0812–0646	J0808–0751 (f)	1.837	2.600	–0.29	S04	40.2	21.2	25.4	1.34
J0828+0508	J0831+0429,0829+046 (b)	0.18	1.225	0.0	S02	33.5	20.2	15.7	1.47
J0829+2413	J0830+2410,0827+243 (f)	0.94	0.713	0.00	S02	111.0	23.7	24.9	1.42
J0845+7049	J0841+7053,0836+710 (f)	2.22	1.757	0.42	S02	33.4	14.2	10.2	1.62
J0852–1216	J0850–1213 (b)	0.57	0.625	–0.37	S04	44.4	44.4	14.0	0.58
J0853+1941	J0854+2006,0851+202 (b)	0.31	2.997	–0.3	S02	15.8	11.3	10.6	1.03
J0917+4427	J0920+4441,0917+449 (f)	2.18	1.368	–0.1	S02	33.5	13.9	13.8	1.19
J0952+5501	J0957+5522,0954+556 (f)	0.90	1.498	0.39	S02	47.2	6.8	9.1	1.12
J0958+6533	J0958+6533,0954+658 (b)	0.37	1.269	–0.3	S02	18.0	14.6	6.0	1.08
J1009+4855	(1011+496) (b)	0.20	0.252	0.21	S02	12.9	6.8	4.8	0.90
J1052+5718	J1058+5628,1055+567 (b)	0.14	0.189	0.09	S02	16.1	7.5	5.0	1.51

Table 1 (Continued)

3EG	ID (f,b)	z	$F_{8.4}$/Jy	$\alpha_{\rm R}$	Ref.	$N_{\gamma{\rm max}}$	$N_{\gamma{\rm min}}$	$N_{\gamma{\rm ave}}$	$\alpha_{\rm G}$
J1104+3809	J1104+3812,1101+384 (b)	0.03	0.631	0.0	S02	27.1	9.0	13.9	0.57
J1133+0033	J1133+0015 (f)	1.17	0.119	0.35	S02	52.2	12.3	3.7	1.73
J1133+0033	J1133+0040 (f)	1.63	0.320	0.05	S02	52.2	12.3	3.7	1.73
J1200+2847	J1159+2914,1156+295 (f)	0.73	1.233	0.24	S02	163.2	12.2	7.5	0.98
J1222+2841	J1221+2813,1219+285 (b)	0.10	1.217	–0.2	S02	53.6	10.8	11.5	0.73
J1224+2118	J1224+2122,1222+216 (f)	0.44	1.073	0.34	S02	48.1	10.8	13.9	1.28
J1229+0210	J1229+0203,1226+023 (f)	0.16	41.725	0.04	S02	48.3	27.8	15.4	1.58
J1236+0457	J1231+0418 (f)	1.03	0.302	0.05	S02	15.2	8.7	6.5	1.48
J1236+0457	J1239+0443,1237+0459 (f)	1.75	0.290	0.09	S02	15.2	8.7	6.5	1.48
J1246–0651	J1248–0632 (f)	0.762	0.353	0.02	S04	44.1	12.9	9.8	1.73
J1246–0651	J1246–0730 (f)	1.286	0.630	–0.08	S04	44.1	12.9	9.8	1.73
J1255–0549	J1256–0547 (b)	0.538	15.600	–0.2	S04	267.3	9.3	74.2	0.96
J1310–0517	J1312–0424 (f)	0.824	0.286	–0.15	S04	23.6	6.6	7.9	1.34
J1314–3431	J1316–3338 (f)	1.210	1.100	0.07	S04	31.8	16.2	14.6	1.28
J1323+2200	J1321+2216 (f)	0.94	0.323	0.0	S02	68.4	16.8	5.2	0.86
J1323+2200	J1327+2210,1324+224 (f)	1.40	2.107	–0.5	S02	68.4	16.8	5.2	0.86
J1329+1708	J1333+1649,1331+170 (f)	2.09	0.483	–0.1	S02	33.1	13.3	4.4	1.41
J1339–1419	J1337–1257 (b)	0.539	3.850	–0.21	S04	20.2	11.8	5.5	1.62
J1347+2932	J1343+2844 (f)	0.91	0.192	0.13	S02	21.0	21.0	9.6	1.51
J1409–0745	J1408–0752 (f)	1.494	0.630	0.00	S04	128.4	28.7	27.4	1.29
J1424+3734	J1419+3821 (f)	1.83	0.775	–0.1	S02	20.9	16.9	10.9	2.25
J1424+3734	J1420+3721 (f)	0.97	0.158	0.06	S02	20.9	16.9	10.9	2.25
J1424+3734	J1421+3855 (f)	0.49	0.132	–0.2	S02	20.9	16.9	10.9	2.25
J1424+3734	J1426+3625 (f)	1.09	0.613	–0.2	S02	20.9	16.9	10.9	2.25
J1500–3509	J1457–3539 (f)	1.422	0.606	0.04	S04	29.5	12.5	10.9	1.99
J1512–0849	J1512–0905 (f)	0.360	2.150	0.12	S04	49.4	25.6	18.0	1.47
J1517–2538	J1517–2422 (b)	0.049	1.930	0.02	S04	37.2	24.2	8.4	1.66
J1527–2358	J1532–2310 (f)	2.289	0.158	–0.09	S04	94.4	37.2	3.3	1.67
J1605+1553	J1603+1554 (f)	0.11	0.256	–0.5	S02	42.0	17.1	12.8	1.06
J1605+1553	(1604+159) (b)	0.36	0.2235	0.56	S02	42.0	17.1	12.8	1.06
J1608+1055	J1608+1029,1606+106 (f)	1.23	1.805	–0.1	S02	62.4	21.0	25.0	1.63
J1614+3424	J1613+3412,1611+343 (f)	1.40	3.042	0.13	S02	68.9	38.8	26.5	1.42
J1625–2955	J1626–2951 (f)	0.815	2.250	0.00	S04	321.8	14.8	47.4	1.07
J1626–2519	J1625–2527 (f)	0.786	1.100	0.45	S04	82.5	20.9	21.3	1.21
J1634–1434	J1628–1415 (f)	1.025	0.275	0.14	S04	69.9	13.5	11.5	1.15
J1635+3813	J1635+3808,1633+382 (f)	1.81	2.448	0.04	S02	107.5	31.8	58.4	1.15
J1727+0429	J1728+0427,1725+044 (f)	0.29	0.622	0.04	S02	27.5	18.1	17.9	1.67
J1733–1313	J1733–1304 (b)	0.902	5.110	0.07	S04	104.8	35.8	36.1	1.23
J1733+6017	J1722+6105 (f)	2.06	0.203	–0.1	S02	22.9	22.9	8.7	2.00
J1738+5203	J1740+5211,1739+522 (f)	1.38	1.318	–0.2	S02	41.3	14.6	18.2	1.42
J1744–0310	J1743–0350 (f)	1.054	6.240	–0.84	S04	48.7	36.0	11.7	1.42
J1824+3440	J1826+3431 (f)	1.81	0.289	0.25	S02	28.7	28.7	4.1	1.03
J1828+0142	J1826+0149 (f)	1.77	0.725	–0.2	S02	132.2	29.1	8.3	1.76
J1832–2110	J1832–2039 (f)	0.103	1.070	0.03	S04	99.3	43.0	26.6	1.59
J1832–2110	J1833–2103 (f)	2.510	6.750	0.25	S04	99.3	17.8	26.6	1.59
J1911–2000	J1911–2006 (f)	1.119	2.190	0.11	S04	31.5	17.6	17.5	1.39
J1911–2000	J1911–1921 (f)	0.804	0.182	0.06	S04	31.5	17.6	17.5	1.39
J1937–1529	J1935–1602 (f)	1.460	0.286	0.04	S04	55.0	22.0	3.7	2.45
J1937–1529	J1939–1525 (f)	1.657	0.670	0.0	S04	55.0	22.0	3.7	2.45
J1959+6342	J2006+6424,2005+6416 (f)	1.57	0.958	–0.3	S02	25.3	18.7	13.3	1.45

Table 1 (Continued)

3EG	ID (f,b)	z	$F_{8.4}$/Jy	$\alpha_{\rm R}$	Ref.	$N_{\gamma\rm max}$	$N_{\gamma\rm min}$	$N_{\gamma\rm ave}$	$\alpha_{\rm G}$
J2006–2321	J2005–2310 (f)	0.830	0.230	0.14	S04	44.1	32.7	7.3	1.33
J2025–0744	J2025–0735 (f)	1.388	0.727	0.33	S04	74.5	30.5	21.2	1.38
J2027+3429	J2025+3343 (f)	0.22	2.728	–0.4	S02	99.3	31.0	25.9	1.28
J2036+1132	J2031+1219 (f)	1.22	1.178	–0.1	S02	35.9	21.8	13.3	1.83
J2036+1132	J2034+1154 (f)	0.61	0.216	0.24	S02	35.9	21.8	13.3	1.83
J2036+1132	(2032+107) (b)	0.60	0.463	0.46	S02	35.9	21.8	13.3	1.83
J2158–3023	J2158–3013 (b)	0.117	0.204	0.44	S04	30.4	15.3	13.2	1.35
J2202+4217	J2202+4216,2200+420 (b)	0.07	3.321	0.31	S02	39.9	18.4	11.1	1.60
J2206+6602	J2208+6519,2206+650 (f)	1.12	0.249	0.33	S02	30.8	20.5	24.4	1.29
J2209+2401	J2212+2355,2209+236 (f)	1.13	0.719	–0.1	S02	45.7	23.1	6.9	1.48
J2232+1147	J2232+1143,2230+114 (f)	1.04	2.923	0.48	S02	51.6	26.9	19.2	1.45
J2254+1601	J2253+1608,2251+158 (f)	0.86	10.380	0.10	S02	116.1	24.6	53.7	1.21
J2255+1943	J2253+1942,2250+1926 (f)	0.28	0.362	–0.10	S02	62.2	14.6	5.8	1.36
J2358+4604	J0004+4615 (f)	1.81	0.214	–0.3	S02	42.8	16.4	14.3	1.38
J2358+4604	J2354+4553,2351+456 (f)	1.99	0.990	0.34	S02	42.8	16.4	14.3	1.38
J2359+2041	J0001+1914 (f)	3.10	0.504	–0.3	S02	26.3	12.8	8.3	1.09
J2359+2041	J0003+2129 (f)	0.45	0.269	–0.6	S02	26.3	12.8	8.3	1.09
J2359+2041	J0004+2019 (f)	0.68	0.162	–0.6	S02	26.3	12.8	8.3	1.09
J2359+2041	J2358+1955,2356+196 (f)	1.07	0.558	0.10	S02	26.3	12.8	8.3	1.09

Notes to Table 1:

a) f/b: b=BL Lac objects, f=FSRQs.
b) $N_{\gamma\rm max}$, $N_{\gamma\rm min}$, $N_{\gamma\rm ave}$: Reference of H99.
c) References: SE02: Sowards-Emmerd et al. (2002); SE04: Sowards-Emmerd et al. (2004); H99: Hartman R. C. et al. (1999).
d) 3EG: J0412-1853, J0542–0655, J1504–1537, J1527–2358, J1921–2015, J1937–1592, J2321–0328, J0215+1123, J1127+4302, J1828+0142, J1824+3440: $N_{\gamma\rm ave}$ =P1234/2; J0852–1216: $N_{\gamma\rm ave}$=P1; J1424+3734: $N_{\gamma\rm ave}$=P12.

observed γ photon flux are converted to flux densities at 1 GeV according to the formula

$$\mathrm{d}N/\mathrm{d}E = N_0 E^{-\alpha_{\rm ph}}, \tag{1}$$

with $\alpha_{\rm ph}$ the photon spectral index given in the 3rd catalog of EGRET (Hartman et al. 1999) and we obtain

$$F_{\rm 1GeV}({\rm Jy}) = 6.64 \times 10^{-(12+\alpha_{\rm G})} \times \alpha_{\rm G} \times N_\gamma^{\rm ob}, \tag{2}$$

$F_{\rm 1GeV}$ (Jy) being the γ-ray flux density at 1 GeV in units of Jy, $\alpha_{\rm G}$ the γ-ray spectral index, and

$$\alpha_{\rm G} = \alpha_{\rm ph} - 1. \tag{3}$$

Here $N_\gamma^{\rm ob}$ is observed photons flux (photon cm^{-2} s^{-1}). The flux densities are k-corrected according to

$$F_\nu = F_\nu^{\rm ob}(1+z)^{\alpha_\gamma - 1}, \tag{4}$$

where α_γ is the spectral index at frequency ν, and z is the redshift.

2.3 Analysis results

We made a linear regression analysis, and obtained the following results.

1) In the low state, no relations showed up for any group (see Table 2). It means either that there is no correlation between γ-ray at 1 GeV and radio flux density at 8.4 GHz, or the correlation is extremely weak when the source is in the low state.

2) In the high state, good correlations are shown for the whole sample and the FSRQ sample, but a weak correlation is shown for the BL Lacs:

For the whole sample (119 blazars):

$$\log F_\gamma = (0.16 \pm 0.06) \log F_{8.4\,\mathrm{GHz}} - (10.64 \pm 0.04), \tag{5}$$

with a correlation coefficient of $r = 0.249$ and a chance probability $p = 0.6\%$ (see Fig. 1).

For FSRQs:

$$\log F_\gamma = (0.19 \pm 0.06) \log F_{8.4\,\mathrm{GHz}} - (10.59 \pm 0.05), \tag{6}$$

with $r = 0.286$ and $p = 0.5\%$ (see Fig. 2).

For BL Lacs:

$$\log F_\gamma = (0.25 \pm 0.14) \log F_{8.4\,\mathrm{GHz}} - (10.80 \pm 0.08), \tag{7}$$

with $r = 0.371$ and $p = 8.9\%$ (see Fig. 3).

Table 2 Liner Regression Analysis Results for Flux Densities

sample	State	C_0	ΔC_0	C_1	ΔC_1	r	SD	p	N	f	b
	High	–10.644	0.041	0.160	0.058	0.249	0.350	0.006			
whole blazars	Lower	–11.058	0.026	0.028	0.037	0.069	0.224	0.453	119	97	22
	average	–11.167	0.036	0.242	0.051	0.399	0.312	<0.0001			
	High	–10.593	0.048	0.187	0.064	0.286	0.340	0.005			
97 FSRQs	Lower	–11.029	0.030	0.056	0.041	0.140	0.216	0.173	97	97	0
	average	–11.144	0.043	0.259	0.058	0.418	0.304	<0.0001			
	High	–10.795	0.078	0.249	0.139	0.371	0.356	0.089			
22 BL Lac	Lower	–11.129	0.056	–0.011	0.099	–0.024	0.254	0.917	22	0	22
	average	–11.228	0.077	0.246	0.138	0.370	0.353	0.090			

Notes to Table 2: The linear regression equations are obtained by $\log F_\gamma = (C_1 \pm \Delta C_1) \log F_{8.4\,\mathrm{GHz}} + (C_0 \pm \Delta C_0)$; r is the correlation coefficient and p is the chance probability; N, f and b are numbers of the sources.

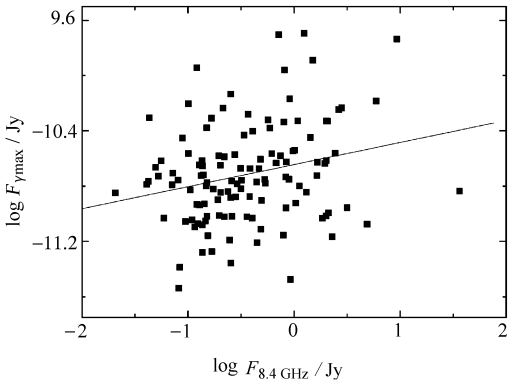

Fig. 1 Plot of the maximum γ-ray data vs radio flux density for the whole simple (119 blazars).

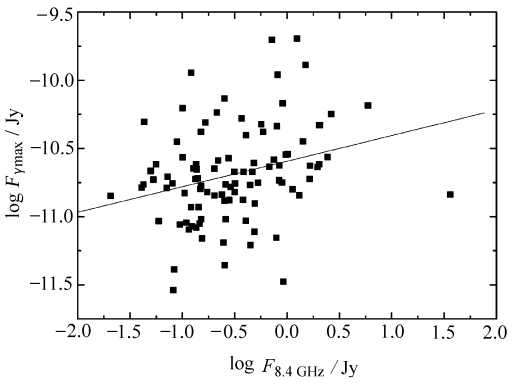

Fig. 2 Plot of the maximum γ-ray data vs radio flux density for the simple of 97 FSRQs.

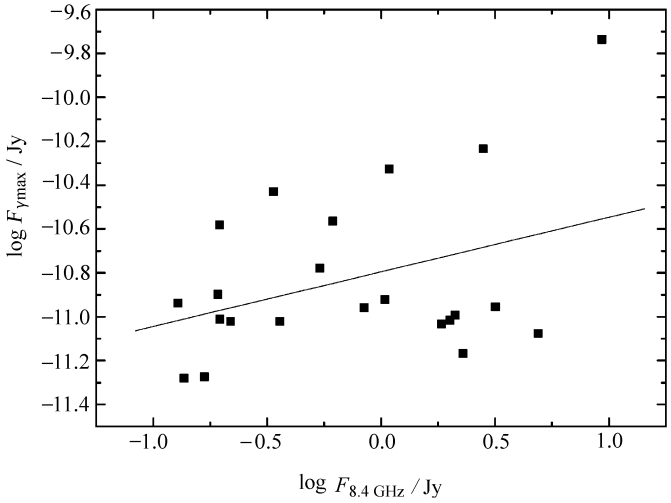

Fig. 3 Plot of the maximum γ-ray data vs radio flux density for the simple of 22 BL Lac objects.

3) For the average data, we obtain following results:
For the whole sample:

$$\log F_\gamma = (0.24 \pm 0.05) \log F_{8.4\,\mathrm{GHz}} - (11.17 \pm 0.04), \tag{8}$$

with $r = 0.40$ and $p < 0.01\%$.

For FSRQs:

$$\log F_\gamma = (0.26 \pm 0.06) \log F_{8.4\,\mathrm{GHz}} - (11.14 \pm 0.04), \tag{9}$$

with $r = 0.42$ and $p < 0.01\%$.

For BL Lacs:

$$\log F_\gamma = (0.25 \pm 0.14) \log F_{8.4\,\mathrm{GHz}} - (11.23 \pm 0.08), \tag{10}$$

with $r = 0.37$ and $p = 9.0\%$. All the results are shown in Table 2.

3 DISCUSSION

The correlation between the γ-ray and radio flux densities has been studied by some authors. Zhou et al. (1997) found that the γ-ray emission is a correlated with the radio core emissions. Fan et al. (1998) checked the correlation between the γ-ray and the 230 GHz bands. They found that, for the maximum data, the γ-ray emission is more closely correlated with the high frequency (1.3 mm, 230 GHz) radio emission than with the lower frequency (5 GHz, 6 cm) radio emission. Schachter & Elvis (1993) reported that there is a correlation between the γ-ray and 5 GHz radio emissions. A good correlation between the radio and γ-ray luminosities for the γ-ray-loud blazars was found by Dondi & Ghisellini (1995). However, Mücke et al. (1997) analyzed the correlation between the radio and γ-ray luminosity in details and found no correlation, but Cheng et al. (2000) and Zhang et al. (2002) found that there is correlation between them. So, there are serious debates on the correlation. The causes for the differences may be 1) that the samples are small, 2) that there is a selected effect caused by the emission data, since there were no simultaneous data for the γ-ray and the radio bands, different choices of the radio and γ-ray emission would naturally result in different conclusions. Therefore, it is necessary to use a large sample and a reasonable choice of data to revisit the correlation.

In this paper, we studied the correlation between the γ-ray and radio flux densities at 8.4 GHz. 1) we used a larger sample than the previous papers; 2) We analysed separately for the maximum, minimum and average γ-ray fluxes; 3) The radio data are from a survey at 8.4 GHz. Our results are: 1) There is no correlation between the γ-ray and radio emission for the lower γ-ray data state; 2) There is a correlation between the γ-ray flux and radio emission for both the maximum and the average flux densities.

The correlations between the γ-ray and radio emissions for high state and average data are much better than that for lower state data. The radio flux densities used here are taken from a survey, and can be taken as the average data for the whole sample. The correlations between high and average γ-ray emissions and radio emission probably suggest that the γ-rays are from the SSC process or that the emissions in the radio and γ-ray bands are strongly beamed.

The blazars are extremely variable when they are in the high state (Fan 2004), this violent variability is caused by the beaming effect (Lainela et al. 1999). So, the γ-ray high state corresponds to strongly beaming. The radio emissions are also beamed. In the beamed case the observed flux density $F^{\rm ob}$ and the intrinsic flux density $F^{\rm in}$ follow the relation $F^{\rm ob}$=$F^{\rm in}\delta^{3+\alpha}$, with δ the Doppler factor and α the spectral index. So for the observed γ-ray flux we have $F_\gamma^{\rm ob} \sim F_\gamma^{\rm in}\delta_\gamma^{3+\alpha_{\rm G}}$, while for radio emission we have $F_{\rm R}^{\rm ob} \sim F_{\rm R}^{\rm in}\delta_{\rm R}^{3+\alpha_{\rm R}}$. Strong beaming (ie., large δ_γ and $\delta_{\rm R}$) will result in an apparent correlation between the γ-ray and radio emissions. Besides, if the γ-ray emissions are from the SSC process, there should be a correlation between the γ-ray and radio emissions.

The γ-ray sources are detected when they are bright, therefore, the average data should behave like the high state data and we should expect a correlation for the average γ-ray data.

Since the radio emission is on average in a bright state, it is in a different state from the low state γ-ray emission, and we can expect no correlation between them. However, we can expect a correlation between the γ-ray and radio emissions in the low state if SSC is responsible for the γ-ray emission. Unfortunately, the 8.4 GHz survey did not give any low state values for many of the sample.

In 1998, Fan et al. considered a sample of 44 objects and obtained a correlation between the radio and γ-ray bands. Later, Zhang et al. (2002) and Zhang et al. (2003) also found the correlation based on the luminosity function. Our results are consistent with theirs.

Our investigation and discussion suggest 1) that the γ-rays are associated with the radio emissions from the jet; 2) that the γ-ray emission is likely from the SSC process in this case; and 3) that, furthermore, data of simultaneous observations are important for the correlation analysis.

Acknowledgements This work is supported partially by the National 973 project (NKBRSF G19990754), the National Science Fund for Distinguished Young Scholars (10125313), and the Fund for Top Scholars of Guangdong Province (Q02114). We also think the Guangzhou City Education Bureau, which supports our research in astrophysics.

References

Blandford R. D., Levinson A. 1995, ApJ, 441, 79
Catanese M., Akerlof C. W., Bradbury S.M., et al. 1998, ApJ, 501, 616
Cheng K. S., Ding W. K. Y., 1994, A&A, 288, 97
Cheng K. S., Zhang X., Zhang L., 2000, ApJ, 537, 80
Dermer C. D., Schlickeiser R., Mastichiadis A., 1992, A&A, 256, L27
Dondi L., Ghisellini G., 1995, MNRAS, 273, 583
Fan J. H., 2004, ChJA&A, in the 5th Microquasar Workshop
Fan J. H. 1997, Ap&SS, 246, 119

Fan J. H. et al., 1998, A&A, 338, 27
Fichtel C. E., Bertsch D. L., Chiang J. et al. 1994, ApJS, 94, 551
Hartman R. C. 1996, ASP Conf. Ser., 110, p.33
Hartman R. C., Bertssch D. L., Bloom A. W. et al., 1999, ApJS, 123, 79
Kühr H., Witzel A., Pauliny-Toth I. I. K., Nauber U., 1981, A&AS, 45, 367
Lainela M., Takalo L. O., Sillanpää A. et al., 1999, ApJ, 521, 561
Mannheim K., Biermann P. L., 1992, A&A, 253, L21
Maraschi L., Ghisellini G., Celotti A., 1992, ApJ, 397, L5
Mücke A., Pohl M., Reich P. et al., 1997, A&A, 320, 33
Punch M. et al., 1992, Nature, 358, 477
Quinn J. et al., 1996, ApJ, 456, L83
Schachter J., Elvis M., 1993, ApJS, 92, 623
Sowards-Emmerd D., Romani R. W., Michelson P. F., 2002, astroph/0212504
Sowards-Emmerd D., Romani R. W., Michelson P. F., 2004, astroph/0403692
Thompson D. J., Bertsch D. L., Dingus B. L. et al., 1995, ApJS, 101, 295
Von Montigny C., Bertsch D. L., Chiang J. et al. 1995, ApJ, 440, 525
Zhang X., Cheng K. S., Zhao G. et al., 2003, Chin. Phys. Lett., 20(7), 1183
Zhang L., Fan J. H., Cheng K. S., 2002, PASJ, 54, 159
Zhou Y. Y., Lu Y. J., Wang T. G. et al. 1997, ApJ, 484, L47